J. Vis. Commun. Image R. 20 (2009) 293–300

Contents lists available at ScienceDirect

J. Vis. Commun. Image R.

journal homepage: www.elsevier.com/locate/jvci

Variational denoising of partly textured images

Fang Li [a], Chaomin Shen [b], Chunli Shen [a], Guixu Zhang [b,*]

[a] Department of Mathematics, East China Normal University, Shanghai 200241, China
[b] Department of Computer Science, East China Normal University, Shanghai 200241, China

ARTICLE INFO

Article history:
Received 25 July 2008
Accepted 27 January 2009
Available online 1 February 2009

Keywords:
Variational denoising
Total variation
Texture detecting function
Local feature

ABSTRACT

The Rudin–Osher–Fatemi model is a widely used variational denoising algorithm which favors piecewise constant solutions. Although edge sharpness and location are well preserved, some local features such as textures and small details are often diminished with noise simultaneously. This paper aims to better preserve these local features using a similar variational framework. We introduce a texture detecting function according to the derivatives of the noisy textured image. Then this function is used to construct a spatially adaptive fidelity term, which adjusts the denoising extent in terms of the local features. Numerical results show that our method is superior to the Rudin–Osher–Fatemi model in both signal-to-noise ratio and visual quality. Moreover, part of our results are also compared with other state-of-the-art methods including a variational method and a non local means filter. The comparison shows that our method is competitive with these two methods in restoration quality but is much faster.

1. Introduction

Image denoising is one of the fundamental problems in image processing. The aim of image denoising is to smooth out noise in an image without losing significant features such as edges and textures.

Variational denoising methods are popular in recent years. The basic variational models are the Perona–Malik model [21] and the Rudin–Osher–Fatemi (ROF) model [23]. The denoising problem can be expressed as follows: Given an image $f : \Omega \subset R^2 \to R$ corrupted by additive zero mean Gaussian noise n with standard deviation σ, the aim is to recover the true image u from

$$f = u + n.$$

In the variational framework, the ROF model can be formulated as finding

$$\min \int_\Omega |\nabla u|\,dx \text{ subject to } \int_\Omega (f-u)^2\,dx = |\Omega|\sigma^2.$$

One can introduce a Lagrange multiplier λ and rewrite the above problem as

$$\min\left\{E(u) = \int_\Omega |\nabla u|\,dx + \frac{\lambda}{2}\int_\Omega (u-f)^2\,dx\right\}. \tag{1}$$

The corresponding Euler–Lagrange equation is

$$\operatorname{div}\left(\frac{\nabla u}{|\nabla u|}\right) + \lambda(f-u) = 0.$$

Neumann boundary condition is assumed. Then λ can be computed by

$$\lambda = \frac{1}{|\Omega|\sigma^2}\int_\Omega \operatorname{div}\left(\frac{\nabla u}{|\nabla u|}\right)(u-f)\,dx. \tag{2}$$

The first term in the energy $E(u)$ in (1) is the so called total variation (TV) regularization term, and the second term is a fidelity term with scalar coefficient λ. Numerically, the solution of (1) is usually achieved by the steepest descent method:

$$\begin{cases} \frac{\partial u}{\partial t} = \operatorname{div}\left(\frac{\nabla u}{|\nabla u|}\right) + \lambda(f-u), \\ u|_{t=0} = f. \end{cases} \tag{3}$$

The ROF model does a good job in image denoising since it preserves edge location and sharpness while smoothing out noise, especially for cartoon like images. The ROF model and its extensions are widely studied numerically and theoretically [2,7,8,18]. It should be mentioned that images are always assumed in the Bounded Variation (BV) space since this space allows discontinuities in functions.

However, the ROF model favors piecewise constant solutions and therefore often causes staircase effects [9,25,26]. Here the staircase effects means that smooth regions with noise are processed into piecewise constant regions. Meanwhile, in Eq. (3) the fidelity coefficient λ is a global scalar, not local, which leads to the effect that the restoration is better achieved in some regions of the image than in others. Then small details and textures are often smoothed out with noise in this process. So the ROF model

* Corresponding author.
E-mail address: gxzhang@cs.ecnu.edu.cn (G. Zhang).

1047-3203/$ - see front matter © 2009 Elsevier Inc. All rights reserved.
doi:10.1016/j.jvcir.2009.01.003

cannot achieve well equilibrium between cartoon like regions and texture like regions when dealing with partly textured images.

In order to overcome the staircase effect, the weighted ROF model and high order PDEs (typically fourth-order PDEs) [9,10,12,17] have been introduced. Meanwhile, many efforts have been tried to improve the results when denoising partly textured images. The one most related to our work is [13,14]. In [13,14] Gilboa et al. introduced local variance constraints instead of the global variance constraint in (1), and then used Lagrange multipliers to convert the problem into an unconstrained energy minimization problem:

$$\min\left\{E(u)=\int_\Omega |\nabla u|\,dx+\frac{1}{2}\int_\Omega \lambda(x)P_R(x)\,dx\right\},$$

where $P_R(x)$ is the local variance. Results in [14] show improvements in the signal-to-noise ratio (SNR) over the original scalar ROF model, while keeping important textures. In [4] the authors used a set of constraints λ_i, here each one corresponds to a region O_i in the image. Their model involves deblurring and denoising problems and can be written as

$$\min\left\{E(u)=\int_\Omega |\nabla u|\,dx+\frac{1}{2}\lambda_i\int_{O_i}(h*u-f)^2\,dx\right\}.$$

They discussed the existence and uniqueness of solutions of their model. A step further, in [1] a set of constraints λ_{ij} is used, and each one corresponds to a pixel of the image. That is to find

$$\min\left\{E(u)=\int_\Omega |\nabla u|\,dx+\sum \lambda_{i,j}\Big(G*(h*u-f)^2(i,j)-\bar{\sigma}^2\Big)\right\},$$

where h is the point spread function and G is a Gaussian kernel. Uzawa algorithm is used to solve the minimization problem. In [25,26], the concept of feature scale is introduced and how the ROF model works with a fixed λ is deeply studied. Based on the local feature scale, in [16] the authors modified the regularization term and obtained the following equation:

$$\left(\frac{s(x)}{s_{\max}}\right)\operatorname{div}\left(\frac{\nabla u}{|\nabla u|}\right)+\lambda(f-u)=0,$$

where s is a local feature scale. However, the scheme to measure local feature scale is rough. In [11], spatial coherence structure is introduced into the regularization process of the Mumford–Shah model through a proper spatially varying function. Different from these local methods, some non local models are also good at denoising textured image. Non-local means (NL-means) filter [6] shows good performance in denoising images with textures and small details. Its idea is to construct a non local weight function $w(x,y)$ for

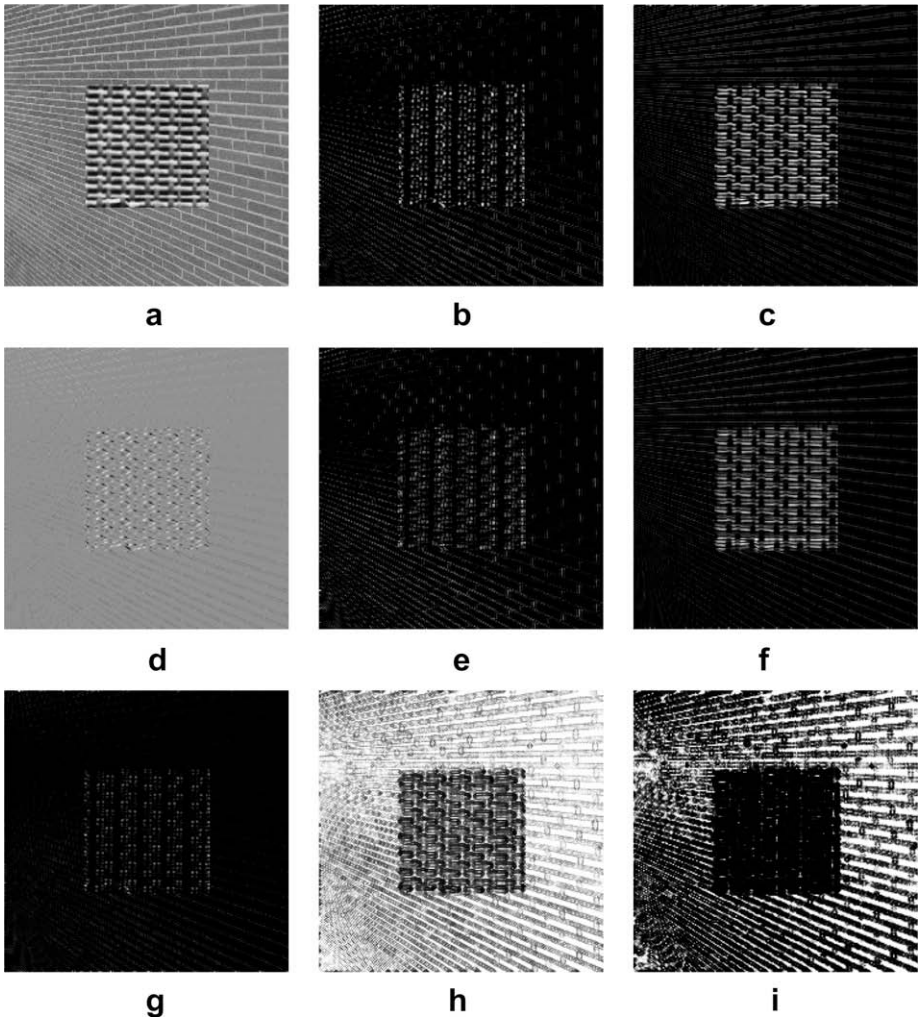

Fig. 1. Example of vector u with six components defined in (5) and two texture detecting functions. (a) Original textured image; (b)–(g) the six components u_1, u_2, u_3, u_4, u_5 and u_6, respectively; (h) the texture detecting function using the first three channels; and (i) the texture detecting function using six channels.

each x, $y \in \Omega$ by the grey level differences in a whole Gaussian neighborhood of x and y, that is

$$w(x,y) = \exp\left(-\frac{1}{h^2}\int_{R^2} G_a(t)|f(x+t) - f(y+t)|^2\,dt\right)$$

where G_a is a Gaussian kernel with standard deviation a and h is a parameter. Then the NL-means filter estimates the value of x by

$$\mathrm{NL}(f)(x) = \frac{\int_\Omega w(x,y)f(y)\,dy}{\int_\Omega w(x,y)\,dy}.$$

In [15], non-local TV is proposed for image regularization in a variational framework.

The above models are almost $BV + L_2$ type. Recently, many studies suggest new norms to substitute L_2 norm in the fidelity term, such as G and H^{-1} norms [3,19,20,24,27]. They can better distinguish cartoon and oscillating parts. In these models, a scalar λ for fidelity term as the ROF model is usually used. Our denoising model as well as the above mentioned spatially varying λ models can also be introduced into these decomposition schemes.

In this paper, with the aim to better preserve both structural and textural information, we modify the fidelity term using a texture detecting function g. Based on the recognition that textures can be distinguished by different feature channels of the image, we introduce a texture detecting function using the first and second derivatives of the smoothed version of the noisy textured image. Then similar to [14], we use the texture detecting function to adjust the fidelity extent in denoising process.

Our paper is organized as follows. In Section 2, we introduce our proposed model in two steps: texture detection and noise removal. Then the numerical implementation details are given in Section 3. In Section 4, we display our experimental results and conduct some comparisons. Finally, we conclude our paper in Section 5.

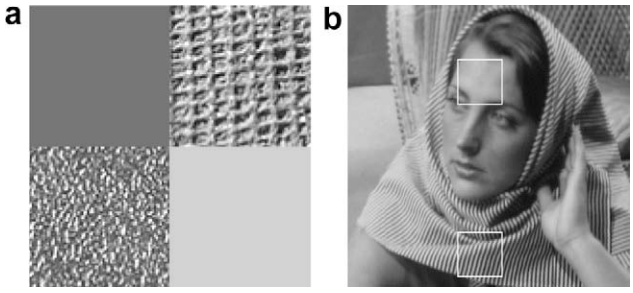

Fig. 2. Partly-textured test images. (a) Synthetic mosaic made of patches of fabric and metal textures with two constant patches as used in [14]. (b) Barbara image. The marked two small regions will be compared by different algorithms in the text.

2. The proposed method

As in Section 1, we assume that f is the observed noisy image. Our denoising method is the combination of two steps. The first step is texture detection and the second step is noise removal. In the following, we use (x,y) to denote the spatial variable.

2.1. Texture detection

The original structure tensor [5] is defined as

$$J_\rho = \begin{pmatrix} G_\rho * (f_x^2) & G_\rho * (f_x f_y) \\ G_\rho * (f_x f_y) & G_\rho * (f_y^2) \end{pmatrix}$$

where G_ρ is a Gaussian kernel with standard deviation ρ and subscripts of f denote partial derivatives to extract the feature of the observed image. Here ρ is a scale parameter. The structure tensor is a powerful tool to discriminate textures. In [22], the structure tensor is used to extract feature in textured images and then these feature channels are taken as initial information to segment the image with textures. Inspired by this idea, we propose to extend the structure tensor by using first and second-order derivatives to extract the texture feature in an image. The major problem of the original structure tensor is the dislocation of edges due to the smoothing with Gaussian kernels. The basic idea in [5] to address this problem is the replacement of the Gaussian smoothing by nonlinear diffusion.

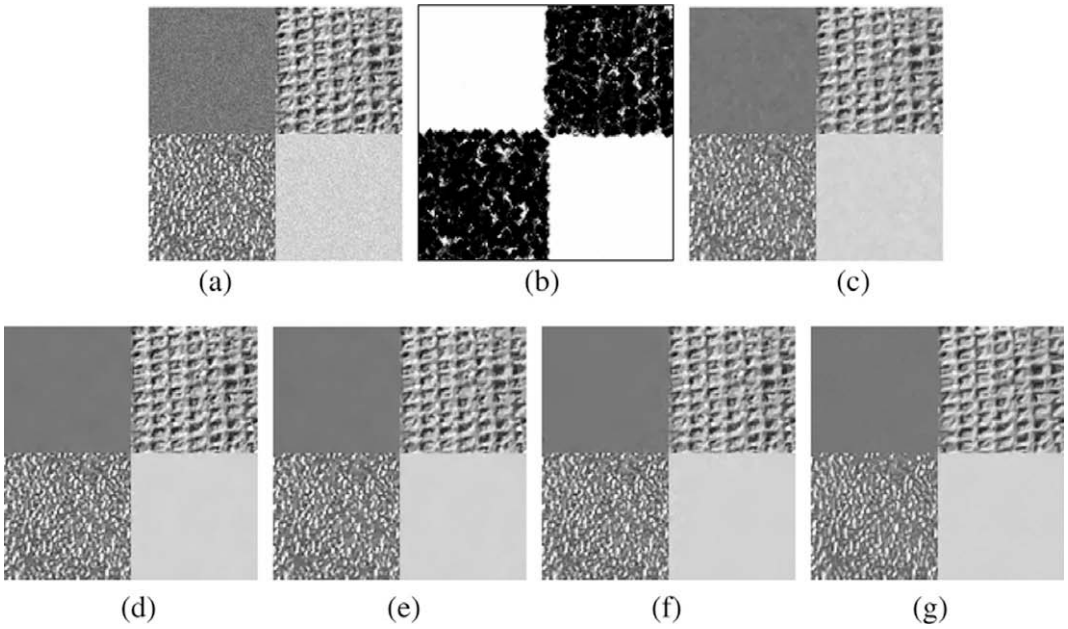

Fig. 3. Denoising result of a noisy mosaic of textures and constant value areas. (a) Mosaic image contaminated by zero mean Gaussian noise with standard deviation $\sigma = 10$, SNR = 14.4 dB; (b) our texture detecting function using six channels of u; (c) result of the ROF model, SNR = 14.6 dB, $t = 2.5$ s; (d) result of our method using six channels of u, SNR = 17.5 dB, $t = 3.2$ s; (e) result of our method using the first three channels of u, SNR = 16.6 dB, $t = 2.9$ s; (f) result of Gilboa et al.'s method, SNR = 16.6 dB, t = 9.8 s; and (g) result of the NL-means filter, SNR = 12.6 dB, $t = 55$ s.

Following [22], we use total variation (TV) flow to smooth the feature channels since it can well preserve edges while removing noise.

First, we preprocess the observed noisy image by TV flow:

$$\begin{cases} \frac{\partial I}{\partial t} = \operatorname{div}\left(\frac{\nabla I}{|\nabla I|}\right), \\ I|_{t=0} = f. \end{cases} \tag{4}$$

By this step, we aim to reduce the influence of large noise. With the idea that textures can be distinguished by different derivatives such as the structure tensor, we construct a vector $u = (u_1, u_2, u_3, u_4, u_5, u_6)$ based on the first- and second-order derivatives of the smoothed function I as follows:

$$u_1 = I_x^2, \quad u_2 = I_y^2, \quad u_3 = I_x I_y, \quad u_4 = I_{xx}^2, \quad u_5 = I_{yy}^2, \quad u_6 = I_{xy}^2. \tag{5}$$

This vector contains texture information in different directions. See Fig. 1(b)–(g).

Since the noise in I is amplified by taking derivatives, we again use the TV flow to denoise each component of u, i.e.

$$\frac{\partial u_i}{\partial t} = \operatorname{div}\left(\frac{\nabla u_i}{|\nabla u_i|}\right), \quad i = 1, \ldots, 6 \tag{6}$$

with initial values (5). Then we define our original texture detecting function as

$$g(x,y) = \frac{1}{1 + k\Lambda(x,y)^2}$$

where k is the contrast factor always set to be 0.005 in this paper and $\Lambda(x,y)$ is the largest eigenvalue of the geometric matrix

$$\begin{pmatrix} 1 + \sum_{i=1}^{6} (u_i)_x^2 & \sum_{i=1}^{6} (u_i)_x (u_i)_y \\ \sum_{i=1}^{6} (u_i)_x (u_i)_y & 1 + \sum_{i=1}^{6} (u_i)_y^2 \end{pmatrix}$$

for each point $(x,y) \in \Omega$. In the homogeneous regions of the image, each component of u is near zero such that Λ goes to zero, and then g goes to one; In the regions with textures, at least one component of u is very large such that Λ goes to infinity, and then g goes to zero. This is the behavior of our texture detecting function. Fig. 1(h) and (i) show the texture detecting functions of using the first three channels (first-order derivatives) and six channels (first- and second-order derivatives). It is obvious that with six channels Fig. 1(i) can detect more texture information than Fig. 1(h). In Section 4, we will compare the denoising performance of using texture detecting function with six channels and the first three channels.

2.2. Noise removal

Now we use the texture detecting function to modify the fidelity term in the ROF model. Our model is to minimize the following energy functional:

$$E(v) = \int_\Omega |\nabla v| \, dxdy + \frac{\mu}{2} \int_\Omega (1-g)(v-f)^2 \, dxdy, \tag{7}$$

where μ is a scalar parameter. After computing the Euler–Lagrange equation, we use the steepest descent method to get the evolution equation:

$$\frac{\partial v}{\partial t} = \operatorname{div}\left(\frac{\nabla v}{|\nabla v|}\right) - \mu(1-g)(v-f). \tag{8}$$

By definition, $g \in (0,1]$. In the cartoon like regions, $g \approx 1$, such that the regularization term takes the main role and the noise is removed. In the regions with textures, $g \approx 0$, such that the fidelity term leads a more important role and then the textures will be well preserved. As a whole, the proposed model will keep a good balance between noise removal and texture preservation.

Moreover, our model can reduce the staircase effect which is a flaw of the ROF model. In the ROF model with fixed fidelity coefficient, $1/\lambda$ is the scale parameter [14,26]. According to [26], when processing an image by the ROF model with fixed λ, image features with scale larger than or equal to $1/\lambda$ will be

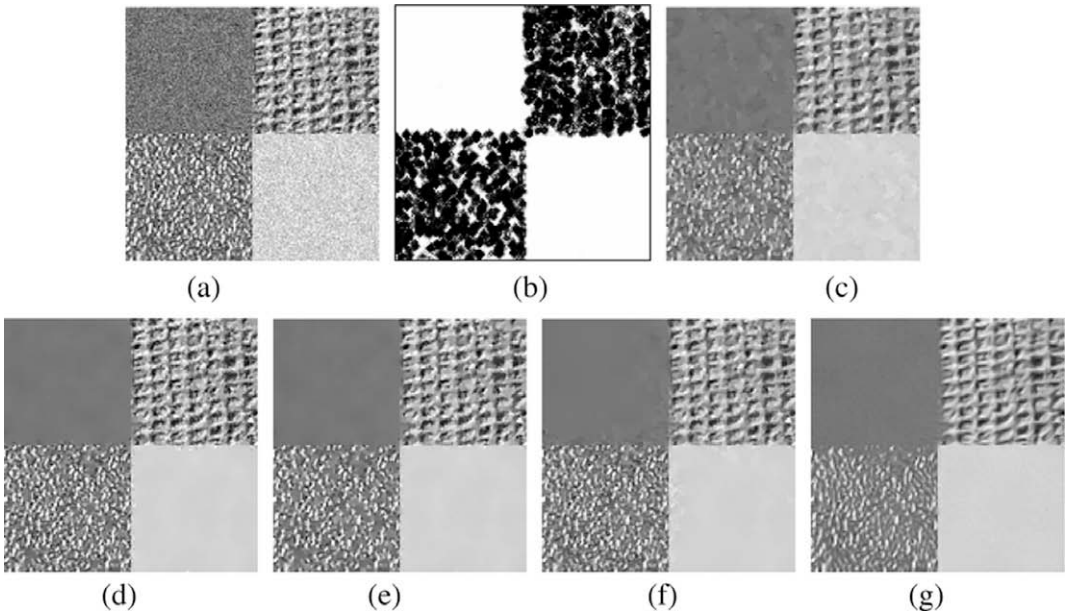

Fig. 4. Denoising of a noisy mosaic of textures and constant areas. (a) Mosaic image contaminated by zero mean Gaussian noise with standard deviation $\sigma = 20$, SNR = 8.1 dB; (b) our texture detecting function using six channels of u; (c) result of the ROF model, SNR = 10.1 dB, $t = 4.0$ s; (d) result of our method using six channels of u, SNR = 11.7 dB, $t = 4.5$ s; (e) result of our method using the first three channels of u, SNR = 11.5 dB, $t = 4.3$ s; (f) result of Gilboa et al.'s method, SNR = 11.7 dB, $t = 22.7$ s; and (g) result of the NL-means filter, SNR = 10.9 dB, $t = 56$ s.

retained while features with scale smaller than $1/\lambda$ will be removed. However, in an image, there are always textures with many scales. A global λ obviously could not adapt all the scales. Meanwhile since the ROF model favors piecewise constant solutions, it causes the staircase effect. In our model, the local fidelity coefficient $\mu(1-g)$ is a function and by definition it is closely related with the textures, so we could expect that it is adapted to many scales locally. Hence the staircase effect can be reduced.

3. Numerical implementation

To discretize Eq. (8), we use finite difference scheme. Denote spatial step size by $h = 1$ and time step size by τ.

$$(D_x^{\pm} v)_{i,j} = \pm[v_{i\pm1,j} - v_{i,j}],$$
$$(D_y^{\pm} v)_{i,j} = \pm[v_{i,j\pm1} - v_{i,j}],$$
$$|(Dv)_{i,j}| = \sqrt{(D_x^{+}(v_{i,j}))^2 + (D_y^{+}(v_{i,j}))^2 + \varepsilon},$$

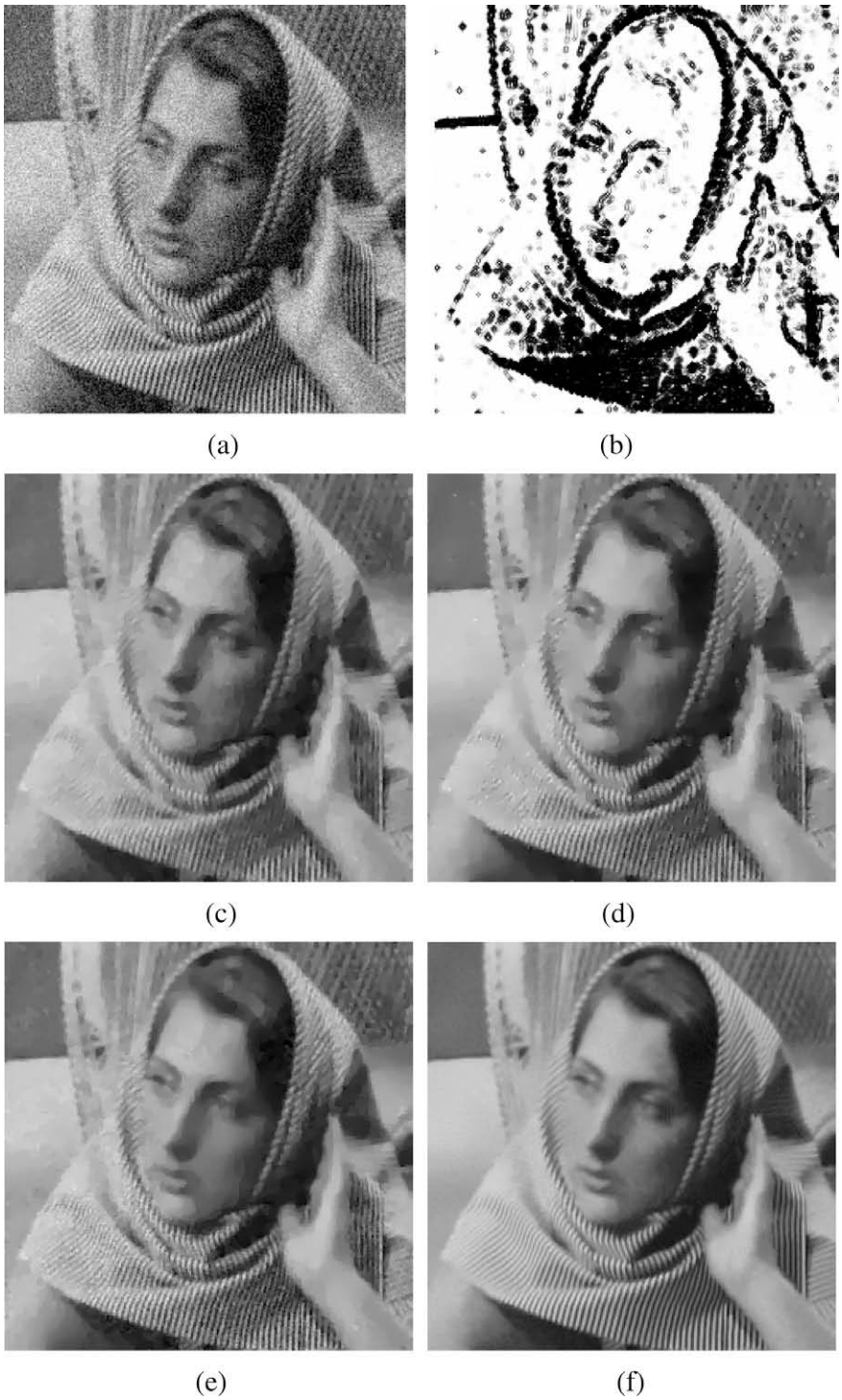

Fig. 5. Denoising of noisy Barbara image. (a) Barbara image contaminated by zero mean Gaussian noise with standard deviation $\sigma = 20$, SNR = 8.1 dB; (b) our texture detecting function; (c) result of the ROF model, SNR = 12.1 dB, $t = 12.4$ s; (d) result of our method, SNR = 13.0 dB, $t = 15.8$ s; (e) result of Gilboa et al.'s method, SNR = 13.2 dB, $t = 129.4$ s; and (f) result of the NL-means filter, SNR = 15.7 dB, $t = 210.0$ s.

where $\varepsilon > 0$ is a small number to avoid dividing by zero. The details of the algorithm for Eq. (8) are given as follows (the subscripts i, j are omitted):

$$v^{k+1} = v^k + \tau D_x^- \left(\frac{D_x^+ v^k}{|Dv^k|} \right) + D_y^- \left(\frac{D_y^+ v^k}{|Dv^k|} \right) - \tau\mu(1-g)(v^k - f).$$

Strong TV flow (4) is implemented similarly. In this paper we set $\tau = 0.2$ when solving (4) and (8). μ is set to be in the range $(0,1]$. By experience, for natural images, $\mu = 0.1$ is a good choice. In this paper, we set $\mu = 0.1$ for all the tests except in Figs. 3 and 4 we set $\mu = 1$. The additive operator splitting (AOS) scheme [28] is used to implement Eq. (6) with time step 5. We only iterate a few times since this algorithm is very fast. For noise level of standard deviation 10–20, one time is enough. For higher noise level, the iteration should be increased. For evolution equations (4) and (8), the stopping criterion is that the difference between the successive iteration is less than a given tolerance or the iteration is larger than a given number. For simplicity, we set the number of iterations as multiple of 10. Generally, the number should be increased as the noise level increases. By trial and error, we find that: for noise level of standard deviation 10, iterating (4) 10 times, iterating (6) one time, and iterating (8) 30 times gives good result; for noise level of standard deviation 20, iterating (4) 60 times, iterating (6) one time, and iterating (8) 100 times yields satisfactory results. For all the test images except Fig. 7 (where the standard deviation of the noise is unknown) in this paper, we use this unified criterion.

In the implementation of the ROF model, we evolve Eq. (3) with automatic varying scalar λ by formula (2) as in [23].

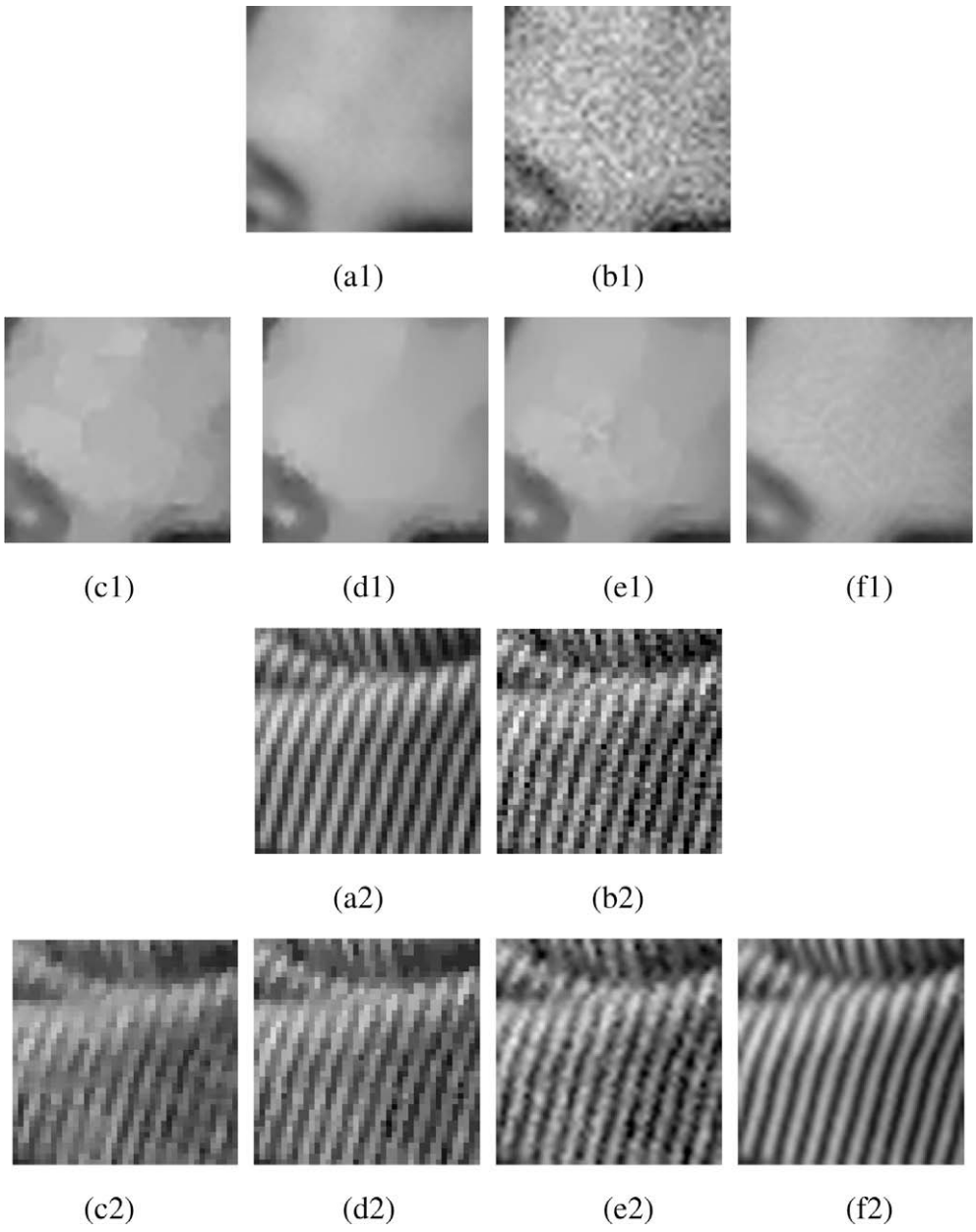

Fig. 6. Two small regions of Barbara image marked in Fig 2(b) are enlarged to make careful comparison with the performance in denoising textures and cartoon. (a1 and a2) Original image regions, one is a typical cartoon region and the other is a textured region; (b1 and b2) noisy image parts; (c1 and c2) results of the ROF model; (d1 and d2) results of our method; (e1 and e2) result of Gilboa et al.'s filter; and (f1 and f2) result of the NL-means method.

4. Experimental results

We test our algorithm with various textured and natural images. Remark that when it is not specified, we use six channels of u in our method. Our method can not only reduce the staircase effect in cartoon like regions but also well preserve textures while removing noise. Our algorithm is compared with the ROF model, Gilboa et al.'s method in [14] and NL-means method in [6] by computational time, signal-to-noise ratio (SNR) and visual quality. The experiments are performed under Windows XP and MATLAB v7.4 with Intel Core 2 Duo CPU at 1.66 GHz and 2 GB memory.

Fig. 2 shows two test images. Fig. 2(a) is a typical partly textured, partly cartoon image with size 148 by 148. Fig. 2(b) is a standard test image Barbara with size 256 by 256. In Figs. 3 and 4, we add zero mean Gaussian noise with standard deviation 10 and 20, respectively, to the mosaic image Fig. 2(a), and compare the denoising results of our method, the ROF model, Gilboa et al.'s method, and the NL-means filter.

Figs. 3(b) and 4(b) show that our texture detection function really can detect the textures, whilst the detecting precision decreases as the noise standard deviation increases. Our denoising results are better than the ROF model in both SNR and visual quality. When the noise standard deviation is 10 or 20, the SNR by our method is remarkably higher than the ROF model. Almost no staircase effect appears in our results which is obvious in the results of the ROF model. For our method, the denoising performance of using six channels u is better than using the first three channels of u. See Figs. 3(d) and (e), Figs. 4(d) and (e), and the corresponding SNRs. Our method is also competitive with Gilboa et al.'s method and NL-means filter. In the case of noise standard deviation 10, our result (Fig. 3(d)) has a SNR higher than Gilboa et al.'s method by 1 dB. In the case of noise standard deviation 20, the SNR of our result (Fig. 4(d)) is similar to the result of Gilboa et al.'s method (Fig. 4(f)). However, in Fig. 4(f), the information of texture invades to the cartoon part in the region near the boundary of cartoon and texture, causing some distortion. Our result (Fig. 4(d)) seems to be more pleasing in this aspect. The results of NL-means method (Figs. 3(g) and 4(g)) seem good for texture part, but they have lower SNR than Gilboa et al.'s method and our method. When the noise is larger, see Fig. 4(g) for example, the cartoon regions are not clean as if there are some small scale textures. It shows in such partly texture images, NL-means method can hardly seek the balance between texture denoising and cartoon denoising. Moreover, our method has the advantage that it is much faster than Gilboa et al.'s method and the NL-means method. The computational time is demonstrated in Figs. 3 and 4. Our method is about three times faster than Gilboa et al.'s method and 10 more times faster than NL-means filter. In Gilboa et al.'s method, the local weight $\lambda(x)$ needs to be updated in the evolution and it depends on the local power which is time consuming. In the NL-means method, the computation of the non local weight $w(x,y)$ is time consuming. Remark that ROF model is faster than ours since our model includes two steps while ROF includes one step similar to our step 2.

In Fig. 5, we display the results of different models on a Barbara image. Zero mean Gaussian noise with standard deviation 20 is added to Fig. 2(b). Our result, Fig. 5(d), has a SNR roughly 1 dB higher than the result of the ROF model (Fig. 5(c)). Gilboa et al.'s method has a similar SNR as our method. NL-means method has the highest SNR among all. However, the computational time of our method is much less than Gilboa et al.'s method and the NL-means method.

In Fig. 6, two small regions, one is piecewise constant region (Fig 6(a1)) and the other is a textured region (Fig 6(a2)), are enlarged for careful comparison. Our method performs better than the ROF model in both regions. In the piecewise constant region of Barbara's forehead, our result avoids the staircase effect and it seems to be the best one among all. It shows in the result of NL-means filter (Fig. 6(f1)) that the cartoon region is not clean as if

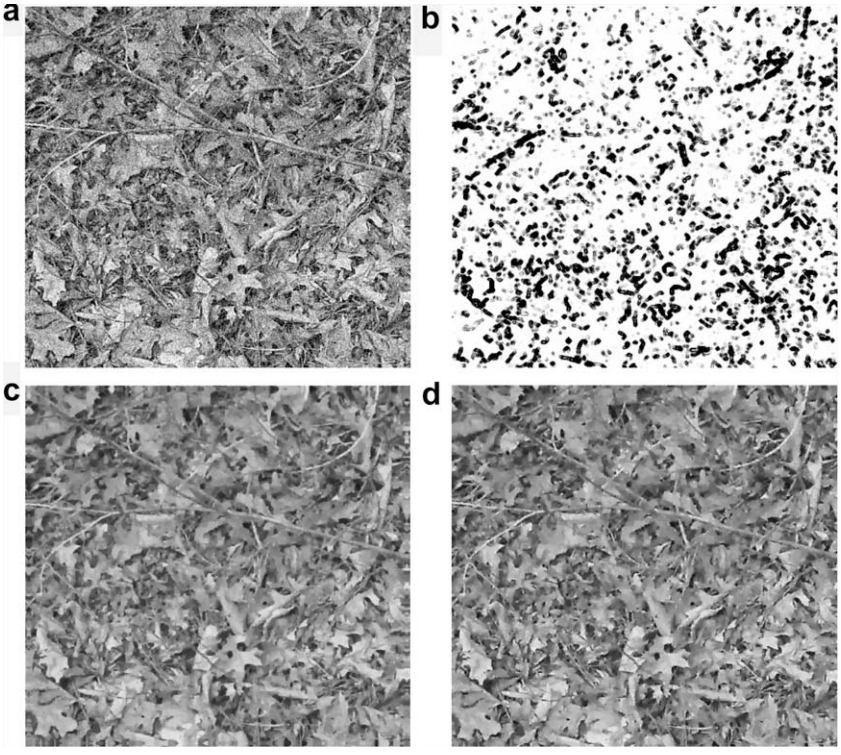

Fig. 7. Denoising of a noisy natural image. (a) Noisy natural image (from http://www.irisa.fr/vista/Themes/Demos/Debruitage/ImageDenoising.html); (b) our texture detecting function; (c) result of the ROF model; and (d) result of our method.

Table 1
More comparison results (dB).

Image	Noisy	ROF	Ours
Cameraman 256	15.9	19.3	20.6
Lena 256	14.3	18.2	19.5
Toys 256	10.0	16.8	17.8
Barboon 512	12.6	12.7	14.3
Bridge 512	14.8	15.8	16.9

there are some small scale textures. In the texture region on the scarf, our result preserves textures better than the ROF model. Meanwhile, our result is similar to Gilboa et al.'s result. The best one is the NL-means method in which the textures are perfectly preserved.

The test on another natural noisy image is displayed in Fig. 7. The given image is a noisy image without knowing the clear image. Since the automatic estimation of λ in the ROF model is based on the known noise standard deviation σ (see formula (2)), we implement the ROF model with a fixed parameter $\lambda = 0.01$ instead. Comparison results show that our model keeps the leaf edges and small details better than the ROF model. We get our result (Fig. 7(e)) by iterating (4) 100 times, iterating (6) two times, and iterating (8) 100 times.

Table 1 shows various natural images and the comparison between the standard ROF model and our proposed method in terms of SNR. From left, SNR of the noisy image; SNR of the ROF model; SNR of our proposed method are showed. All the test images are degraded by zero mean Gaussian white noise with standard deviation $\sigma = 10$. It is clear that our method improves the denoising results.

Denoising result of several classical test images with size 256 by 256 or 512 by 512. From left, SNR of the noisy image; SNR of the ROF model; SNR of our proposed method. All the test images are degraded by zero mean Gaussian white noise with standard deviation $\sigma = 10$.

5. Conclusion

A modified ROF model based on texture detecting function is presented. The proposed algorithm outperforms the standard ROF model in both SNR and visual quality. It can not only better preserve textures but also reduce staircase effect when denoising non-cartoon images in comparison with the standard ROF model. Our method is competitive with the state-of-the-art work by Gilboa et al. and NL-means filter in restoration quality but is much faster than them. Further study will be focused on applying the texture detecting function to other existing variational image processing methods such as denoising, decomposition and deblurring. In Fig 5(b), the textures are not very well captured since there are too many scales in textures. In the future work, a more exact texture detecting function should be constructed by introducing the concept of scale in feature channel construction or using Gabor filter.

Acknowledgments

Fang Li thanks G. Gilboa for his open source code for [14] and A. Buades for his open source code for NL-means filter. This work is supported by the National Basic Research Program (973 Program, No. 2006CB708305), National Science Foundation of China (Nos. 60773119 and 10671066), Ph.D. Program Scholarship Fund of ECNU 2008 (No. 20080037), Shanghai Rising-Star Program (07QH14005) and The Research Fund for the Doctoral Program of Higher Education (200802691037).

References

[1] A. Almansa, C. Ballester, V. Caselles, G. Haro, A TV based restoration model with local constraints, J. Sci. Comput. 34 (2008) 209–236.
[2] G. Aubert, P. Kornprobst, Mathematical Problems in Image Processing, Applied Mathematical Sciences, second ed., vol. 14, Springer, Berlin, 2006.
[3] J.F. Aujol, G. Aubert, L. Blanc-Féraud, A. Chambolle, Image decomposition into a bounded variation component and an oscillating component, J. Math. Imaging Vis. 22 (2005) 71–88.
[4] M. Bertalmio, V. Caselles, B. Rougé, A. Solé, TV based image restoration with local constraints, J. Sci. Comput. 19 (2003) 95–122.
[5] T. Brox, J. Weickert. Nonlinear matrix diffusion for optic flow estimation, in: Proceedings of the 24th DAGM Symposium, Lecture Notes in Computer Science, vol. 2449, Zürich, Switzerland, Springer, Berlin, 2002, pp. 446–453.
[6] A. Buades, B. Coll, J.M. Morel, A review of image denoising methods, with a new one, SIAM Multiscale Model. Simul. 4 (2005) 490–530.
[7] A. Chambolle, P.L. Lions, Image recovery via total variation minimization and related problems, Numer. Math. 76 (1997) 167–188.
[8] Y.M. Chen, M. Rao, Minimization problems and associated flows related to weighted p energy and total variation, SIAM J. Math. Anal. 34 (2003) 1084–1104.
[9] Y.M. Chen, S. Levine, M. Rao, Variable exponent, linear growth functionals in image restoration, Numer. Math. 66 (2006) 1383–1406.
[10] T. Chan, A. Marquina, P. Mulet, High-order total variation-based image restoration, SIAM J. Sci. Comput. 22 (2000) 503–516.
[11] E. Erdem, A. Sancar-Yilmaz, S. Tari, Mumford–Shah regularizer with spatial coherence, in: SSVM, 2007, pp. 545–555.
[12] F. Li, C. Shen, J. Fan, C. Shen, Image restoration combining a total variational filter and a fourth-order filter, J. Vis. Commun. Image Rep. 18 (2007) 322–330.
[13] G. Gilboa, N. Sochen, Y.Y. Zeevi, Texture preserving variational denoising using an adaptive fidelity term, in: Proceedings of the VLSM 2003, Nice, France, 2003, pp. 137–144.
[14] G. Gilboa, N. Sochen, Y.Y. Zeevi, Variational denoising of partly textured images by spatially varying constraints, IEEE Trans. Image Process. 15 (2006) 2281–2289.
[15] G. Gilboa, S. Osher, Nonlocal linear image regularization and supervised segmentation, SIAM Multiscale Model Simul. 6 (2007) 595–630.
[16] J. Hu, H. Wang, Adaptive total variation based on feature scale, Trans. Eng. Comput. Technol. V2 (2004) 245–248.
[17] M. Lysaker, A. Lundervold, X.C. Tai, Noise removal using fourth-order partial differential equation with applications to medical magnetic resonance images in space and time, IEEE Trans. Image Process. 12 (2003) 1579–1590.
[18] M. Lysaker, S. Osher, X.C. Tai, Noise removal using smoothed normals and surface fitting, IEEE Trans. Image Process. 13 (2004) 1345–1357.
[19] Y. Meyer, Oscillatory Patterns in Image Processing and Nonlinear Evolution Equations, University Lecture Series, AMS, 2001. vol. 22.
[20] S. Osher, A. Sole, L. Vese, Image decomposition and restoration using total variation minimization and the H^{-1} norm, SIAM Multiscale Model. Simul. 1 (2003) 349–370.
[21] P. Perona, J. Malik, Scale space and edge detection using anisotropic diffusion, IEEE Trans. Pattern Anal. Mach. Intell. 12 (1990) 629–639.
[22] M. Rousson, T. Brox, R. Deriche, Active unsupervised texture segmentation on a diffusion based feature space, in: Proceedings of the CVPR'03, Madison, WI, 2003, pp. 699–704.
[23] L. Rudin, S. Osher, E. Fatemi, Nonlinear total variation based noise removal algorithms, Physica D. 60 (1992) 259–268.
[24] J.L. Starck, M. Elad, D.L. Donoho, Image decomposition via the combination of sparse representations and a variational approach, IEEE Trans. Image Process. 14 (2005) 1570–1582.
[25] D.M. Strong, T.F. Chan, Edge-preserving and scale-dependent properties of total variation regularization, Inverse Probl. 19 (2003) S165–S187.
[26] D.M. Strong, J.F. Aujol, T.F. Chan, Scale recognition, regularization parameter selection, and Meyer's G norm in total variation regularization, UCLA CAM Report 05-02.
[27] L.A. Vese, S.J. Osher, Modeling textures with total variation minimization and oscillating patterns in image processing, J. Sci. Comput. 19 (2003) 553–572.
[28] J. Weickert, B.M.t.H. Romeny, M.A. Viergever, Efficient and reliable scheme for nonlinear diffusion filtering, IEEE Trans. Image Process. 7 (1998) 398–410.